

Theory of point-contact spectroscopy in electron-doped cuprate superconductors

C. S. Liu^{1,2,*} and W. C. Wu¹

¹*Department of Physics, National Taiwan Normal University, Taipei 11650, Taiwan*

²*Institute of Theoretical Physics, Chinese Academy of Sciences, Beijing 100080, China*

(Received 9 August 2007; revised manuscript received 20 October 2007; published 6 December 2007)

In the hole-doped $d_{x^2-y^2}$ -wave cuprate superconductors, due to the midgap surface state (MSS), a zero-bias conductance peak (ZBCP) is widely observed in [110] interface point-contact spectroscopy (PCS). However, a ZBCP of this geometry is rarely observed in the electron-doped cuprates, even though their pairing symmetry is still likely of the $d_{x^2-y^2}$ wave type. We argue that this is due to the coexistence of antiferromagnetic (AF) and superconducting orders. Generalizing the Blonder-Tinkham-Klapwijk formula to include an AF coupling, it is shown explicitly that the MSS is destroyed by the AF order. The calculated PCS is in good agreement with the experiments.

DOI: 10.1103/PhysRevB.76.220504

PACS number(s): 74.20.-z, 74.25.Ha, 74.45.+c, 74.50.+r

Pairing symmetry is an important issue in the development of an understanding of the mechanism of superconductivity. For hole-doped high- T_c cuprate superconductors, it is generally accepted that the pairing symmetry is $d_{x^2-y^2}$ wave.¹ Among many supporting experiments, point-contact spectroscopy (PCS) measurement shows a zero-bias conductance peak (ZBCP) due to the existing midgap surface state (MSS) in the [110] direction.²⁻⁴ On the electron-doped side of cuprates, although no consensus has been reached yet, more and more recent experiments have found results also consistent with a $d_{x^2-y^2}$ -wave pairing symmetry.⁵⁻¹⁰ Thus one expected to see a similar ZBCP for the electron-doped cuprates. The situation is more subtle than this naive expectation, however. The ZBCP has been consistently observed in underdoped samples. In optimally and overdoped samples, in contrast, two doping-dependent coherence peaks were generally observed.¹¹⁻¹⁴ This has been taken to indicate that the excitation gap in electron-doped cuprates might switch from d to s wave when the doping is increased—a phenomenon consistent with what was observed in magnetic penetration depth measurements.¹⁵

The clues toward an understanding of the complicated PCS of the electron-doped cuprates lie in the doping evolution of the two (often called α and β) pocket Fermi surfaces (FSs) and the nonmonotonic $d_{x^2-y^2}$ -wave excitation gap, as revealed by angle-resolved photoemission (ARPES) measurements.^{6,16} These phenomena have been interpreted in terms of a phenomenological two-band model,¹⁷ which in turn led to a successful account of the magnetic penetration depth measurement¹⁷ and Raman scattering¹⁸ data. The key feature of the two-band model is that the α - and β -band superconducting (SC) gaps are both monotonic $d_{x^2-y^2}$ wave, but with different (doping-dependent) amplitudes. Thus it was originally expected that the [110] MSS should also exist in electron-doped cuprates. The difficulty in describing the experiments suggests that there may be some other physics intervening in the system in the SC state.

The most promising candidate (for this absence) is the coexistence of an antiferromagnetic (AF) order with the SC order. This scenario finds support in ARPES as the data have been well explained in terms of a \mathbf{k} -dependent band-folding effect due to an existing AF order.¹⁹⁻²³ Apart from the ARPES data, no other direct evidence indicates that AF order

does indeed exist in these materials. Therefore, it is highly desirable that some other experiments provide more definitive information regarding the possible existence of AF order in the electron-doped cuprates. When a normal electron is incident into a superconductor, it will induce the excitation of single quasiparticles (QPs) corresponding to all possible orderings. A tunneling experiment is thus considered to be one of the best choices for obtaining this information. Among various tunneling measurements, PCS is one of the most sensitive probes for the electronic states.

In this paper, we shall focus on the effect of AF order on the PCS of a normal-metal–insulator–superconductor (NIS) junction. It will be shown explicitly that the MSS can be destroyed by AF order. The observed PCS on electron-doped cuprates is actually the result of competition between the contributions from AF and SC orders.

Based on the simplest model that captures the essential physics, we will first consider a superconductor overlayer which is coated with a clean, size-quantized, normal-metal overlayer of thickness d , that is much shorter than the mean free path l of normal electrons. The interface is assumed to be perfectly flat and infinitely large. Considering $l \rightarrow \infty$, the discontinuity of all parameters at the interface can be neglected, except for the SC order parameter for which the proximity effect is ignored.² For the $d_{x^2-y^2}$ -wave superconductor of interest, the interface is manipulated to be perpendicular to the \mathbf{k}_x axis (along the [110] direction). When both SC and AF orders exist, QP excitations of an inhomogeneous superconductor have a coupled electron-hole character associated with the coupled \mathbf{k} and $\mathbf{k} + \mathbf{Q}$ [$\mathbf{Q} = (\pi, \pi)$] subspaces. Correspondingly QP states can be described by the generalized Bogoliubov–de Gennes equations²⁴

$$\begin{aligned} Eu_1 &= h_0 u_1 + \Delta_{\mathbf{k}} v_1 + \Phi u_2, \\ Ev_1 &= \Delta_{\mathbf{k}} u_1 - h_0 v_1 + \Phi v_2, \\ Eu_2 &= \Phi u_1 + h_0 u_2 + \Delta_{\mathbf{k}+\mathbf{Q}} v_2, \\ Ev_2 &= \Phi v_1 + \Delta_{\mathbf{k}+\mathbf{Q}} u_2 - h_0 v_2, \end{aligned} \quad (1)$$

where $h_0 \equiv -\hbar^2 \nabla_x^2 / 2m - \mu$ with μ the chemical potential, Φ is the AF order parameter, and $\Delta_{\mathbf{k}}$ ($=\Delta_0 \sin 2\theta$) is the

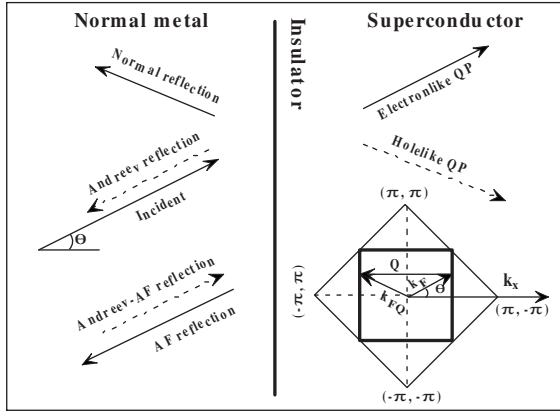


FIG. 1. Schematic plot shows all possible reflection and transmission processes for a normal electron incident into a NIS junction, where AF order exists in the SC side. The inset shows the incident wave vector $\mathbf{k}_F=(k_{x0}, k_y, k_z)$ and its corresponding AF wave vector $\mathbf{k}_F+\mathbf{Q}\equiv\mathbf{k}_{FQ}=(-k_{x0}, k_y, k_z)$ due to AF coupling. Both vectors are tied to the FS, which is approximated by a square (thick line). For convenience, the \mathbf{k}_x axis is chosen to be along the [110] direction.

$d_{x^2-y^2}$ -wave SC order parameter with $\Delta_{\mathbf{k}+\mathbf{Q}}=-\Delta_{\mathbf{k}}$. Here the two-component wave functions u_1 and v_1 are related to \mathbf{k} subspaces, while u_2 and v_2 are related to $\mathbf{k}+\mathbf{Q}$ subspaces. In arriving at Eq. (1), the pairing potential is assumed to be $\sim\Delta_{\mathbf{k}}\Theta(x)$ with $\Theta(x)$ the Heaviside step function² and $\Delta_{\mathbf{k}}$, given above, the Fourier transform of the Cooper pair order parameter in the relative coordinates.

To better describe the effect of an AF order, the FS will be approximated by a square (see Fig. 1). Thus, at nearly half filling, the FS matches the magnetic Brillouin zone (MBZ) boundary. Under the WKBJ approximation²⁵ ($l=1, 2$)

$$\begin{pmatrix} u_l \\ v_l \end{pmatrix} = \begin{pmatrix} e^{i\mathbf{k}_F \cdot \mathbf{r}} \tilde{u}_l \\ e^{-i\mathbf{k}_F \cdot \mathbf{r}} \tilde{v}_l \end{pmatrix} \quad \text{and} \quad \begin{pmatrix} \tilde{u}_l \\ \tilde{v}_l \end{pmatrix} = e^{-\gamma x} \begin{pmatrix} \hat{u}_l \\ \hat{v}_l \end{pmatrix},$$

with γ being the attenuation constant for $|E(\mathbf{k}_F)| < |\Delta(\mathbf{k}_F)|$ and $\mathbf{k}_F=(k_x, k_y, k_z)$, Eq. (1) becomes the Andreev equation in the \mathbf{k}_x direction,

$$E \begin{pmatrix} \hat{u}_1 \\ \hat{v}_1 \\ \hat{u}_2 \\ \hat{v}_2 \end{pmatrix} = \begin{pmatrix} \varepsilon & \Delta_{\mathbf{k}} & \Phi & 0 \\ \Delta_{\mathbf{k}} & -\varepsilon & 0 & \Phi \\ \Phi & 0 & -\varepsilon & -\Delta_{\mathbf{k}} \\ 0 & \Phi & -\Delta_{\mathbf{k}} & \varepsilon \end{pmatrix} \begin{pmatrix} \hat{u}_1 \\ \hat{v}_1 \\ \hat{u}_2 \\ \hat{v}_2 \end{pmatrix}, \quad (2)$$

for the superconducting overlayer ($x>0$). Here $\varepsilon=\varepsilon(k_x)=i\gamma k_x/m$. The wave-vector components parallel to the interface are conserved for all possible processes.

Solving Eq. (2), one obtains eigenvalues $E=\pm\sqrt{\Delta_{\mathbf{k}}^2+\Phi^2+\varepsilon^2}$ where $+$ ($-$) corresponds to the electron- (hole)like QP excitation. Since $\varepsilon(-k_{x0})=-\varepsilon(k_{x0})$ and $\Delta(-k_{x0})=-\Delta(k_{x0})$, states for $k_x=k_{x0}$ and $-k_{x0}$ are actually degenerate. Thus, for $k_x=k_{x0}$, one can have two degenerate eigenstates for electronlike QP excitation, while for $k_x=-k_{x0}$, one can have another two degenerate eigenstates

for electronlike QP excitation. Superposition of these four eigenstates thus gives a formal wave function for the superconductor overlayer,

$$\begin{aligned} \psi_S(x) = & \left[c_1 \begin{pmatrix} \Delta_{\mathbf{k}} \\ E_- \\ 0 \\ \Phi \end{pmatrix} + c_2 \begin{pmatrix} E_+ \\ \Delta_{\mathbf{k}} \\ \Phi \\ 0 \end{pmatrix} \right] e^{-\gamma x} e^{ik_{x0}x} \\ & + \left[c_3 \begin{pmatrix} E_- \\ -\Delta_{\mathbf{k}} \\ \Phi \\ 0 \end{pmatrix} + c_4 \begin{pmatrix} -\Delta_{\mathbf{k}} \\ E_+ \\ 0 \\ \Phi \end{pmatrix} \right] e^{-\gamma x} e^{-ik_{x0}x}. \end{aligned} \quad (3)$$

Here $E_{\pm}\equiv E\pm\varepsilon$ and c_i are the coefficients of the corresponding waves. The wave function $\psi_S(x)$ remains the same if the eigenstates of holelike QP are considered.

Solving Eq. (2) when both $\Delta_{\mathbf{k}}$ and Φ are set to zero, one may obtain bound states to the normal-metal overlayer ($-d<x<0$). In this case, the eigenvalues become $E=\pm k_{x0}k_1/m$, assuming that the incident electron has the wave vector $k_x=k_1$. At the interface, the wave functions of normal metal and superconductor meet ideal continuity $\psi_N(x=0)=\psi_S(x=0)$. One thus obtains the formal wave function for the normal-metal overlayer:

$$\begin{aligned} \psi_N(x) = & \left[c_1 \begin{pmatrix} e^{ik_1x}\Delta_{\mathbf{k}} \\ e^{-ik_1x}E_- \\ 0 \\ e^{ik_1x}\Phi \end{pmatrix} + c_2 \begin{pmatrix} e^{ik_1x}E_+ \\ e^{-ik_1x}\Delta_{\mathbf{k}} \\ e^{-ik_1x}\Phi \\ 0 \end{pmatrix} \right] e^{ik_{x0}x} \\ & + \left[c_3 \begin{pmatrix} e^{-ik_1x}E_- \\ -e^{ik_1x}\Delta_{\mathbf{k}} \\ e^{ik_1x}\Phi \\ 0 \end{pmatrix} + c_4 \begin{pmatrix} -e^{-ik_1x}\Delta_{\mathbf{k}} \\ e^{ik_1x}E_+ \\ e^{ik_1x}\Phi \\ e^{-ik_1x}\Phi \end{pmatrix} \right] e^{-ik_{x0}x}. \end{aligned} \quad (4)$$

Considering the effect of a free boundary at $x=-d$, it requires that $\psi_N(x=-d)=0$. We then obtain the following eigencondition for the surface bound states:

$$e^{-2ik_1d}E_+ + e^{2ik_1d}E_- = 2\Phi. \quad (5)$$

Equation (5) represents one of the major results in this paper. When the AF order $\Phi=0$, there exists a zero-energy state which is responsible for the ZBCP widely observed in hole-doped $d_{x^2-y^2}$ -wave cuprate superconductors.² When $\Phi\neq 0$, the zero-energy state no longer exists so that the energy of the existing state is always finite. It is thus argued that the ZBCP does not exist in a system where the AF and SC orders coexist, and this is the reason for the absence of the ZBCP in the electron-doped cuprates. The above argument remains correct when $d\rightarrow 0$, which corresponds to the case of no normal-metal overlayer (vacuum or an insulating layer).

In order to compare the theory with experiments, we next consider a superconductor [110] surface in point contact with a normal-metal (scanning tunneling microscope) tip. In this

case, a thin insulating layer is considered to exist between the normal metal and the superconductor (see Fig. 1). For this kind of NIS junction, the barrier potential is assumed to be a δ function, $V(x)=H\delta(x)$. Considering that an electron is injected into the interface from the normal-metal side (with an angle θ), four possible reflections and their related coefficients are detailed as follows: (a) Normal reflection (reflected as electrons) with the coefficient r_S ; (b) Andreev reflection (reflected as holes, due to electron and hole coupling in the \mathbf{k} subspace) with the coefficient r_A ; (c) AF reflection (reflected as electrons, due to the \mathbf{k} and $\mathbf{k}+\mathbf{Q}$ subspace coupling) with the coefficient r_{AF}^e ; (d) Andreev AF reflection (reflected as holes, due to electron and hole coupling in the $\mathbf{k}+\mathbf{Q}$ subspace) with the coefficient r_{AF}^h . In terms of these coefficients, the formal wave function for the normal-metal side can then be written as

$$\psi_N(x) = \begin{bmatrix} \exp(ik_{x0}x) + r_S \exp(-ik_{x0}x) \\ r_A \exp(ik_{x0}x) \\ r_{AF}^e \exp(ik_{x0}x) \\ r_{AF}^h \exp(-ik_{x0}x) \end{bmatrix}.$$

The four reflection coefficients are determined by the boundary conditions

$$\psi_N(x)|_{x=0^-} = \psi_S(x)|_{x=0^+},$$

$$\frac{2mH}{\hbar^2} \psi_S(x)|_{x=0^+} = \frac{d\psi_S(x)}{dx} \Big|_{x=0^+} - \frac{d\psi_N(x)}{dx} \Big|_{x=0^-}. \quad (6)$$

The normalized tunneling conductance is then given by

$$\begin{aligned} \tilde{\sigma}(E, \theta) = & 1 - |r_S(E, \theta)|^2 + |r_A(E, \theta)|^2 \\ & + |r_{AF}^e(E, \theta)|^2 - |r_{AF}^h(E, \theta)|^2. \end{aligned} \quad (7)$$

The actual tunneling conductance is intimately determined by the junction properties. When the tip and the superconductor are in an ideal point contact, i.e., when the effective potential barrier $\hat{Z} \equiv 2mH/\hbar^2$ is sufficiently low and narrow, the wave functions at the interface meet the condition of continuity well. Consequently, Andreev and AF reflections are important. For nonideal point contacts, in contrast, only the normal reflection is important. In the following, we focus on the case of a low and narrow barrier, i.e., the PCS.

Since the theory is aimed at the electron-doped cuprates, the issues concerning their doping-dependent AF and SC orders are crucial. Shown in the inset I of Fig. 2(a) is a typical SC gap for electron-doped cuprates. The gap is piecewise: both segments are fitted to the monotonic $d_{x^2-y^2}$ wave ($\Delta_0 \sin 2\theta$), with different amplitudes ($\Delta_{0\beta}$ and $\Delta_{0\alpha}$). The β - and α -band FS segments are characterized by the cutoff angles θ_1 and θ_2 . The values of the doping-dependent θ_1 and θ_2 were extracted from the ARPES data.¹⁶

In a real NIS junction experiment, the total tunneling conductance is given by $\sigma(E) = \int \tilde{\sigma}(E, \theta) d\theta$. Here the integration over the angle between θ_1 and θ_2 is ruled out, since there the FS is absent. In the following, the dimensionless quantities $\Phi_\beta \equiv \Phi/\Delta_{0\beta}$ and $\Phi_\alpha \equiv \Phi/\Delta_{0\alpha}$, which play the determining

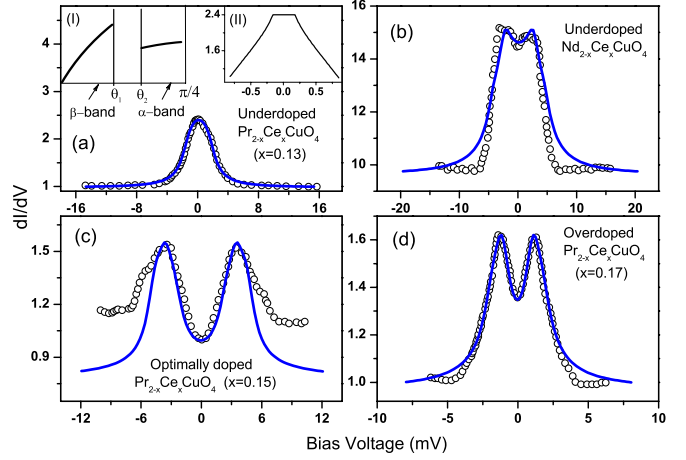


FIG. 2. (Color online) Fitting to the low-resistance G - V data of electron-doped cuprates. Data in (a),(c),(d) are taken from Ref. 26 on $\text{Pr}_{2-x}\text{Ce}_x\text{CuO}_4$ at $T=1.43$ K, while data in (b) are taken from Ref. 12 on $\text{Nd}_{2-x}\text{Ce}_x\text{CuO}_4$. Fitting parameters are summarized in Table I. Inset I in (a) shows a typical piecewise $d_{x^2-y^2}$ -wave gap, with θ_1 (θ_2) characterizing the cutoff angle for β - (α)-band FS. Inset II shows the $\hat{Z} \rightarrow 0$ calculation, emphasizing the zero-bias “peak” structure in (a).

role in the actual PCS, will be given from the fitting calculations. The actual values of Φ , $\Delta_{0\alpha}$, and $\Delta_{0\beta}$ can also be obtained through the fitting processes. Moreover, in the calculation, the QP energy E will be replaced by $E - i\Gamma$ with Γ characterizing the finite lifetime of the QPs. The parameters from the best fittings are summarized in Table I. As a matter of fact, only parameters associated with the β band (i.e., associated with the nodal region) are sensitive to the fitting.

Figure 2(a) compares the theoretical calculations with the conductance-voltage (G - V) curve of PCS data²⁶ on underdoped $\text{Pr}_{2-x}\text{Ce}_x\text{CuO}_4$ (PCCO) ($x=0.13$). For this case, $\hat{Z}=0.05$ is used to simulate a low resistance ($R=9.8 \Omega$). The result is shown to be in good quantitative agreement with the data, for which $(\Phi_\beta, \Phi_\alpha) = (0.1, 0.2)$ are obtained. The smallness of Φ_α and Φ_β indicates that the effect of AF order is unappreciable. As a consequence, a strong ZBCP appears, revealing the dominance of the $d_{x^2-y^2}$ -wave symmetry of the gap. This is in full support of the conclusion drawn in Ref. 26 that the pairing symmetry for the underdoped samples is consistent with $d_{x^2-y^2}$ wave. To explore the AF effect in more detail, the G - V curve is recalculated for an ideal point con-

TABLE I. Three (dimensionless) fitting parameters Φ_β , Φ_α , and \hat{Z} , obtained from Fig. 2. $\Delta_{0\beta}$, $\Delta_{0\alpha}$, and Φ (in units of meV) in the right three columns are determined exclusively from Φ_β and Φ_α together with the actual peak energy. Labels (a)–(d) are referred to those frames in Fig. 2.

| | Φ_β | Φ_α | \hat{Z} | $\Delta_{0\beta}$ | $\Delta_{0\alpha}$ | Φ |
|-----|--------------|---------------|-----------|-------------------|--------------------|--------|
| (a) | 0.10 | 0.20 | 0.05 | 1.88 | 0.94 | 0.19 |
| (c) | 0.75 | 1.00 | 1.50 | 3.00 | 2.25 | 2.25 |
| (d) | 0.70 | 0.75 | 0.75 | 1.33 | 1.24 | 0.93 |
| (b) | 0.70 | 0.90 | 0.25 | 3.33 | 2.59 | 2.33 |

tact ($\hat{Z}, \Gamma \rightarrow 0$). In this limit [see inset II in Fig. 2(a)], the zero-bias “peak” is actually a mix with a narrow plateau. The plateau, which resembles the feature of an s -wave superconductor, arises simply because a small but finite AF order exists near the nodal region.

The evolution of the AF order can be understood from the doping-dependent FS. In underdoped electron-doped cuprates, due to their more distant FS from the MBZ, the scattering about $\mathbf{Q}=(\pi, \pi)$ is weak. This results in a small AF order. With increasing doping, the FS approaches and crosses the MBZ, and the scattering about \mathbf{Q} becomes more important, which leads to a more important AF order.^{21,27} Upon further increase of the doping, long-range order is destroyed, such that the AF order decreases and vanishes eventually.

A similar plateau (with a dip) structure has also been observed in PCS on underdoped $\text{Nd}_{2-x}\text{Ce}_x\text{CuO}_4$.¹² To fit this set of data, $(\Phi_\beta, \Phi_\alpha)=(0.7, 0.9)$ and $\hat{Z}=0.25$ are obtained [see Fig. 2(b)]. Comparing the result with that in inset II of Fig. 2(a), the G - V curve changes from a plateau to a two-peak structure. The latter results from much higher Φ_β and Φ_α and a slightly higher resistance \hat{Z} . The dip at zero bias is evidence that the ZBCP does not exist in this case.

Consider more closely how the FS segments evolve as the doping changes. At low doping, the α -band FS first emerges in the antinodal direction before the superconductivity sets in. When the doping is increased, the β -band FS appears simultaneously with the appearance of superconductivity. Since the MSS is the signature for a superconductor which has symmetrically a positive and a negative portion of the gap, as long as Φ is unappreciable, the ZBCP can still be observed in underdoped samples no matter how the FS segments emerge, or even in the (unrealistic) case without the nodal (β -band) FS.

PCS with high resistance \hat{Z} has been observed on optimally doped PCCO ($x=0.15$).²⁶ In the best fitting [Fig. 2(c)],

large ratios $(\Phi_\beta, \Phi_\alpha)=(0.75, 1.0)$ and $\hat{Z}=1.5$ (for $R=18 \Omega$) are obtained. The strong effect of the AF order Φ leads to a clear two-peak feature, consistent with the case of a dominant s -wave gap. Nevertheless, the theoretical curve deviates from the data at higher biases confirming that a higher \hat{Z} is in use and the wave functions at the interface do not meet the condition of continuity.

In Fig. 2(d), a fairly good fitting is also made with the PCS data on overdoped PCCO ($x=0.17$),²⁶ for which large $(\Phi_\beta, \Phi_\alpha)=(0.7, 0.75)$ and a relatively smaller \hat{Z} (for $R=2.6 \Omega$) are used. Again, a two-peak feature consistent with an s -wave gap manifests the largeness of Φ . In Ref. 26, the G - V curve in Fig. 2(d) was also fitted using the Blonder-Tinkham-Klapwijk model. Various pairing models were tested and it is the $(d+is)$ -wave symmetry that leads to the best result. This does support the scenario discussed in the current paper that single-particle excitation is gapped by both SC and AF orders, $\Delta_{\text{eff}} \equiv |\Delta_d + i\Phi| = \sqrt{\Delta_d^2 + \Phi^2}$. The actual PCS is indeed the competitive result between the SC and AF contributions.

In summary, PCS of the electron-doped cuprates is investigated. It is shown explicitly that the MSS of the d -wave superconductor can be destroyed by the presence of AF order (Φ). Due to the smallness of Φ , a ZBCP occurs in the underdoped sample, consistent with $d_{x^2-y^2}$ -wave pairing. A more important effect of Φ results in a two-peak feature in optimally and overdoped samples. The phenomenon that the peak energy first increases and then decreases as doping increases is soundly explained.

We thank T. Xiang and H. G. Lou for useful comments. This work was supported by the National Science Council of Taiwan (Grant No. 94-2112-M-003-011) and the National Natural Science Foundation of China (Grant No. 10347149). We also acknowledge support from the National Center for Theoretical Sciences, Taiwan.

*Present address: Department of Physics, Yanshan University, Qinhuangdao, China.

¹C. C. Tsuei and J. R. Kirtley, *Rev. Mod. Phys.* **72**, 969 (2000).

²C.-R. Hu, *Phys. Rev. Lett.* **72**, 1526 (1994).

³Y. Tanaka and S. Kashiwaya, *Phys. Rev. Lett.* **74**, 3451 (1995).

⁴G. Deutscher, *Rev. Mod. Phys.* **77**, 109 (2005).

⁵T. Sato *et al.*, *Science* **291**, 1517 (2001).

⁶H. Matsui *et al.*, *Phys. Rev. Lett.* **95**, 017003 (2005).

⁷N. P. Armitage *et al.*, *Phys. Rev. Lett.* **87**, 147003 (2001).

⁸Ariando *et al.*, *Phys. Rev. Lett.* **94**, 167001 (2005).

⁹G. Blumberg *et al.*, *Phys. Rev. Lett.* **88**, 107002 (2002).

¹⁰M. M. Qazilbash *et al.*, *Phys. Rev. B* **72**, 214510 (2005).

¹¹F. Hayashi *et al.*, *J. Phys. Soc. Jpn.* **67**, 3224 (1998).

¹²A. Mourachkine, *Europhys. Lett.* **50**, 663 (2000).

¹³A. Biswas *et al.*, *Phys. Rev. Lett.* **88**, 207004 (2002).

¹⁴L. Shan *et al.*, *Phys. Rev. B* **72**, 144506 (2005).

¹⁵M.-S. Kim *et al.*, *Phys. Rev. Lett.* **91**, 087001 (2003).

¹⁶N. P. Armitage *et al.*, *Phys. Rev. Lett.* **88**, 257001 (2002).

¹⁷H. G. Luo and T. Xiang, *Phys. Rev. Lett.* **94**, 027001 (2005).

¹⁸C. S. Liu *et al.*, *Phys. Rev. B* **73**, 174517 (2006).

¹⁹H. Matsui *et al.*, *Phys. Rev. Lett.* **94**, 047005 (2005).

²⁰C. Kusko *et al.*, *Phys. Rev. B* **66**, 140513(R) (2002).

²¹K.-K. Voo and W. C. Wu, *Physica C* **417**, 103 (2005).

²²Q. Yuan *et al.*, *Phys. Rev. B* **73**, 054501 (2006).

²³D. Sénéchal *et al.*, *Phys. Rev. Lett.* **94**, 156404 (2005).

²⁴P. G. de Gennes, *Superconductivity of Metals and Alloys* (Benjamin, New York, 1966).

²⁵J. Bardeen *et al.*, *Phys. Rev.* **187**, 556 (1969).

²⁶M. M. Qazilbash *et al.*, *Phys. Rev. B* **68**, 024502 (2003).

²⁷K. Yamada *et al.*, *Phys. Rev. Lett.* **90**, 137004 (2003).